Alexandre Humberto Andrei: GAIA and a New Optical Reference Frame, IVS 2006 General Meeting Proceedings, p.10–19
http://ivscc.gsfc.nasa.gov/publications/gm2006/andrei

GAIA and a New Optical Reference Frame

Alexandre Humberto Andrei

Observatório Nacional/MCT and Observatório do Valongo/UFRJ
e-mail: oat1@on.br

Abstract

The ESA mission GAIA, currently scheduled for launch in mid-2011 for a 5-year-mission, will repeatedly measure the position of nearly one billion stars to perform a statistically complete galactic census, carrying out astrometric, spectroscopic and multi-band photometric observations. The target position precision is 10μas at V=15 and 50μas at V=18. To translate such precision into astrometric accuracy, a primary frame formed by some 10,000 quasars will be used, recognized through the analysis of the satellite observation capabilities outputs themselves.

1. Overview

The ESA mission GAIA was initially named as an acronym for "Global Astrometry for Astrophysics". In this sense the astrometry performed, which will refer to a primary frame formed by quasars, is tailored towards the main astrophysics objective, namely a statistically complete census of the Galaxy. The astrometry, in turn, depends on the instrument and mission characteristics.

It is therefore instructive to list the mission's overall goals and scientific objectives. The most relevant among them include: (a) Mapping of the Milky Way; (b) Stellar physics (classification, masses, luminosities, temperatures, metalicities); (c) Kinematics and Dynamics of the Galaxy; (d) Distance scales (trigonometric parallaxes to 10 kpc, cepheids and RR Lyr calibration); (e) Age of the Universe (Cluster diagrams, distances, luminosity); (f) Dark matter (through potential tracers); (g) Reference frames (both primary defined by quasars and extended using stellar astrometry); (h) Extra-solar planets (Jupiter class, astrometric and photometric method); (i) Fundamental physics (PPN parameters, and constraints on the rate of change of the gravitational constant and on gravitational wave energy); (j) Solar system (Taxonomy, Masses, Orbits, and the discovery of new bodies).

The launch is scheduled for mid-2011, using a Soyuz launcher, for a mission of 5 years. The mission is an all sky survey at the end of which about 1 billion objects will be observed to obtain a statistically complete census of the Galaxy, and also of Solar System and extragalactic sources, up to the 20^{th} magnitude (Perryman, 2003a). For objects of the 15^{th} magnitude the astrometric precision can attain 10μas. Besides the astrometric ones, the observational capabilities include photometry (5 broad bands and 11 medium bands), radial velocity, and spectroscopy (low precision). Figure 1 shows the mission's timeline and orbital placement.

In the next two sections we present a review of the astrometric and, to a lesser extent, photometric capabilities that are going to be used to define the GAIA primary reference frame, followed by a discussion of the construction of the primary frame itself. In this sense this paper collects the efforts of several researchers connected to the mission, to whom our debt and appreciation are acknowledged from the start.

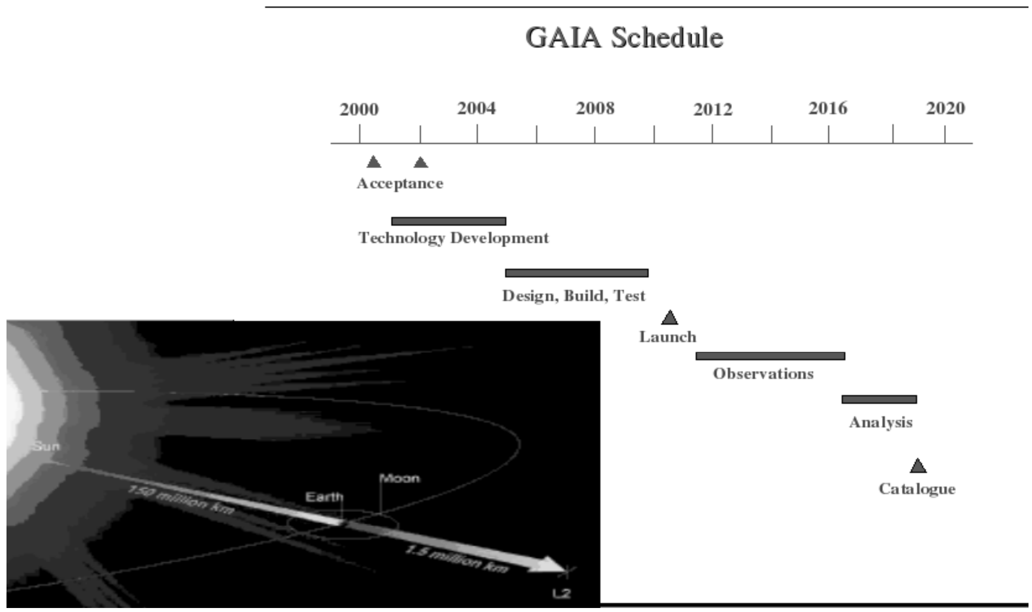

Figure 1. GAIA mission timeline. The detail shows an illustration of the L2 Lagrange point, around which the satellite Lissajous will orbit avoiding the Earth's shadow.

2. The ASTRO Instrument

The GAIA payload includes two astrometric ('Astro') telescopes separated by a basic angle of 106°, with a common focal plane, and radial velocity spectrometer and photometric instrument integrated in the 'Spectro' telescope, that precedes the Astro telescopes by 38° and 144°. Notice that the Astro telescopes also do broad band photometry. These primary instruments are supported by the opto-mechanical-thermal assembly consisting of (Perryman, 2003b): (i) a single structural torus supporting all mirrors and focal planes, employing silicon carbide for both mirrors and structure— there is a symmetrical configuration for the two astrometric viewing directions, with the Spectro system accommodated within the same structure; (ii) a deployable sunshield to avoid direct Sun illumination and rotating shadows on the payload module, combined with the solar array assembly; (iii) control of the heat injection from the service module into the payload module, and control of the focal plane assembly power dissipation in order to provide an ultra-stable internal thermal environment; (iv) an alignment mechanism on the secondary mirror for each astrometric instrument, with micron-level positional accuracy to correct for telescope aberration and mirror misalignment at the beginning of life; (v) a permanent monitoring of the basic angle, but without active control, on board. Figure 2 illustrates the payload assembly.

The integrated radial velocity spectrometer and photometric Spectro instrument comprises an all-reflective three-mirror telescope of aperture 0.5×0.5 m^2 and focal length 2.3m. The mirrors will be coated with Aluminum for enhanced performance in the near ultra-violet. The field of view is separated into a dedicated Sky Mapper, the radial velocity spectrometer, and an 11-medium-band-filters photometer (Katz, 2003).

The Spectro instruments share the Sky Mappers, that consists of two first columns of pixels (with another two columns duplication further up) to detect, confirm, and classify the entering

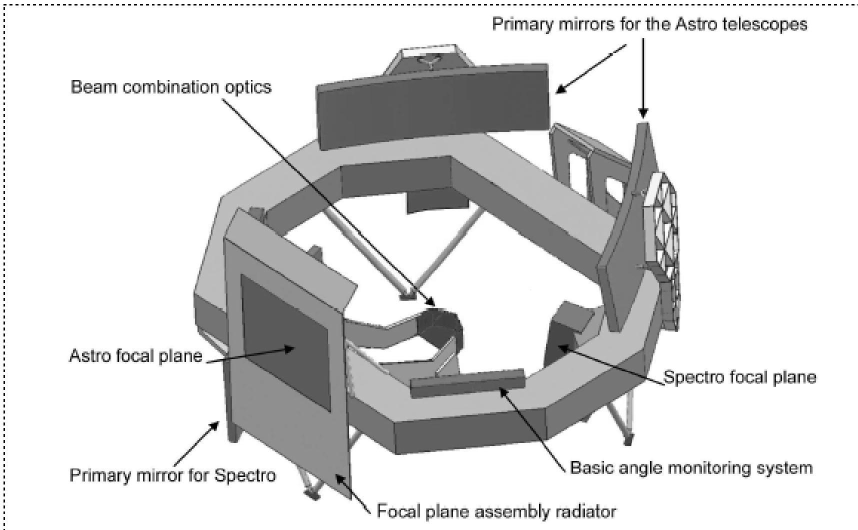

Figure 2. Schematic illustration of the GAIA payload. There is no deployable element (except for the sunshield, not shown in the figure). Note that the structure and mirrors are made of thermally stable SiC.

objects and to determine the operating windows to follow each transit, since not all pixels can be transmitted to ground due to telemetry demands. The Radial Velocity Spectrometer has as primary objective the acquisition of radial velocities to complement the proper motion measurements provided by Astro. The wavelength range is 848 to 874nm, with a resolving power of 1/11500 and a precision of 15 to 1km/s from the faint end to the bright end. It will provide the radial velocities of about 250 million stars up to the 18^{th} magnitude, collecting on average 100 spectra per star over the mission period (Katz, 2003, 2005). The medium band photometry instrument covers 11 medium bands using 8 blue-sensitive and 7 red-sensitive CCDs. The CCDs operate in time delay integration (TDI) mode, and the spatial resolution is 1×1.5 arcsec (i.e., $10 \times 15\mu$m pixels, along and across scan). Several bands measure the continuum while others are located on spectral features sensitive to luminosity, metallicity, element abundances, and H_α emission. Besides the stellar astrophysics results, the photometric measurements will play an all important part in the quasar recognition, particularly those that will form the primary reference frame (Jordi, 2003c).

All along the 5-year-mission the Astro instrument will obtain relative positions, from its two telescopes, for objects brighter than magnitude G=20 (which translates to Johnson V=21 for V-I=2.0, and V=20.5 for V-I=1.0). The overall optical path of each astrometric telescope is made of six anastigmatic, silver-coated reflectors, two of which are common for the two telescopes, to a focal length of 46.67m. The aperture is $1.4 \times 0.5\text{m}^2$. The two telescopes are separated by the 106° basic angle, and the two fields of view of $0.94° \times 0.74°$ are superimposed on the focal plane (Perryman, 2003c). Figure 3 brings details of the Astro focal plane.

The two first columns of the Astro focal plane contain the Sky Mappers (one for each telescope). They detect the objects entering the field of view, and communicate details of the transit to the subsequent astrometric and broad band photometric detectors. Real-time and telemetry bandwidth constraints impose a stern process of detection, confirmation, and selection of the sources that will actually be tracked. The scan is made within an observation window of 6×12 pixels or 12×12 pixels, respectively, for sources fainter or brighter than magnitude 16 (Lindegren, 2005). The

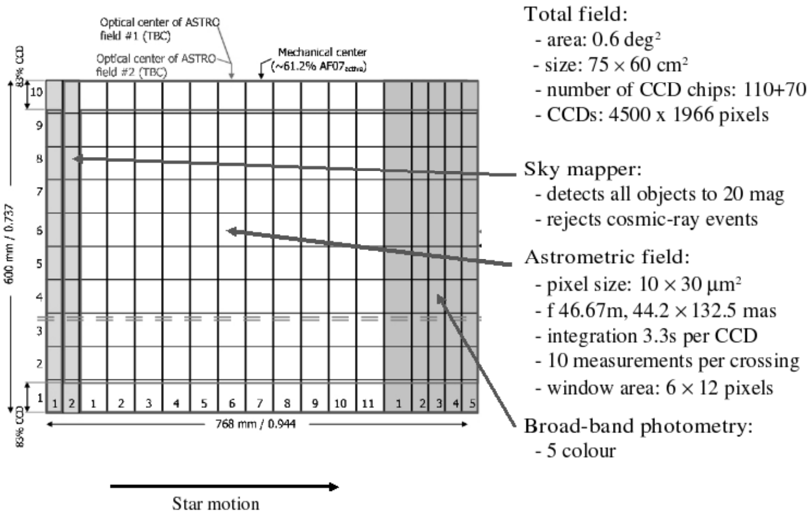

Figure 3. Schematics of the Astro focal plane. The points highlighted on the right are further developed in the text (Jordi, 2003a).

CCDs in the astrometric field sample the optical image (source brightness convolved with the point-spread function) in the along-scan direction by binning the charges across scan in a small read-out vector centered on the image detected in the Sky Mappers. Along scan, these vectors will be 6 or 12 samples wide and only these samples are transmitted to the ground. The astrometric field consists of 11 columns by 10 rows of CCDs (Arenou, 2003; Hog, 2003). Next is the broad band photometry field. In Figure 3 the so-called 2B system proposal is shown which has five bands covering the spectral region from 350 to 1050nm.

The resulting focal plane design consists of a mosaic of 180 CCDs with pixels of 10μm along scan $\times$ 30μm across scan size (44.2 mas $\times$ 132.6 mas). The sources are tracked in Time Delay Integration (TDI) mode. The same CCD design is used for the entire focal plane, with the only difference in the number of pixels along scan (2600 or 4500) and minor changes in the operating modes depending on the assigned functions. The size of the CCDs and the entire focal plane yields TDI and average end-of-mission integration times of 3.3 and 3175 seconds (supposing 82 transits), respectively (Jordi, 2003b).

The integration times naturally depend also on the satellite scanning law. GAIA will perform its observations from a controlled Lissajous-type orbit around the L2 Lagrange point of the Sun and Earth-Moon system (Mignard, 2005a). During its 5-year operational lifetime the satellite will continuously spin around its axis, with a constant speed of 60 arcsec/sec. As a result a great circle in the sky is swept in 6h, and a same field is seen by the two Astro telescopes with 106min of difference. GAIA's spin axis slowly precesses around the solar direction with a fixed angle of 50°, defined for thermal stability. The precession period is of 72 days, corresponding to 26 revolutions over the 5 years of the mission. As a result of the movements of spinning and revolution, on average, each object on the sky is observed 83 times (astrometric fields combined) (de Bruine, 2003a).

Just as was done for the Hipparcos mission, the measurements of the along scan distance between the mesh of objects enables to define instrumental corrections (e.g., satellite attitude and

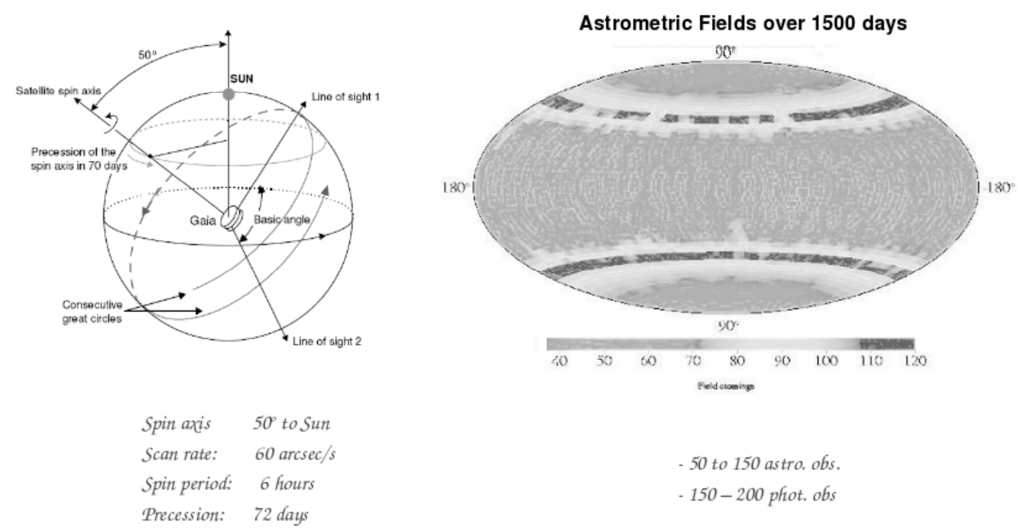

Figure 4. On the left, an illustration of the satellite attitude and varying orientation. On the right, a plot indicating in ecliptic coordinates the number of observations per region of the sky. Notice that the two darker strips of highest concentration of observations around 50° from the ecliptic plane are quite narrow, showing the evenness attained for the number of observations.

telescopes separation), to compute the objects' motion, and ultimately to establish a reference frame on the celestial sphere. Together with the properties of its optical and detector systems, the scanning law and mission lifetime determine GAIA's astrometric capabilities. The scanning law is chosen in such a way to maximize the uniformity of the end-of-mission sky coverage. In spite of this, the characteristics of the scanning law imply that the astrometric precision varies with direction on the sky. Moreover, for any given direction, there is a significant difference between attainable position, proper motion, and parallax accuracy. Generally, end-of-life position and proper motion (random) errors will be 20 per cent and 50 per cent smaller than end-of-life parallax (random) errors. The properties of GAIA's optical and detector systems are such that for stars brighter than $V=12^{th}$ magnitude the photon noise is negligible. The end-of-mission astrometric accuracies for these stars will amount to a few μas, the so-called accuracy noise floor. For magnitudes between 12 and 20, photon noise determines that the expected end-of-life astrometric accuracies are about 10 to 20 μas at V=15 and a few hundred μas at V=20 mag. At a given magnitude (e.g. V=15 mag), the astrometric precision also depends on the apparent star color and on the quantum efficiency of the CCDs and the transmission of the optics. Figure 5 shows the varying precision relatively to magnitude and color (de Bruine, 2003b).

3. GAIA Primary Reference Frame

As seen, GAIA's mode of operation was chosen so that a highly coherent astrometric frame results from the combination of the more than 80 observations of each of the 1 billion objects in different subsets and orientation. The residual global rotation (w) of the frame can be removed by fitting the apparent proper motion of extragalactic sources. By restricting these objects only to QSOs and AGNs for the sake of pointlikeness, a quasi-inertial reference frame is built, in the sense

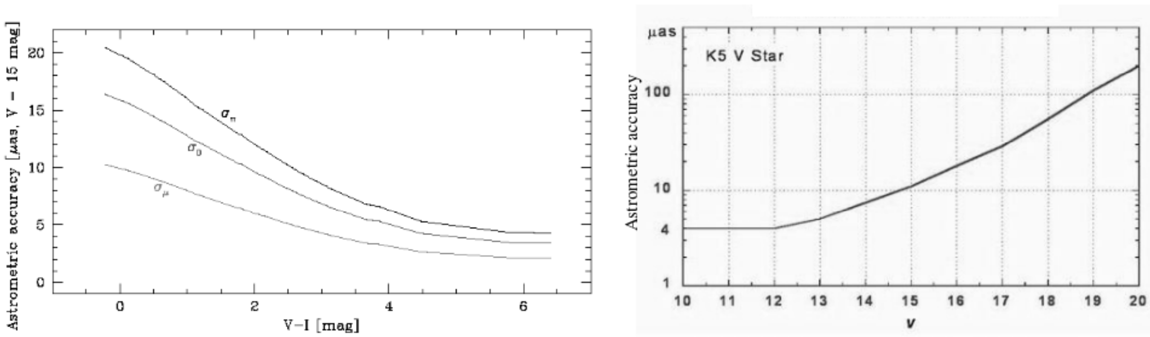

Figure 5. On the left, the variation of accuracy with color. For same conditions of magnitude, color and sky location, notice the increasing accuracy in the sense parallax to position and to proper motion. On the right, the variation of accuracy with magnitude, exemplified by a K5V star.

of the ICRF. Through this a direct realization of the ICRS is obtained in the optical domain, with an average individual astrometric accuracy of not worse than 100μas for hundreds of thousands of grid points. Figure 6 gives an account of the expected number of quasars. The components of w can be obtained from a selected sample, i.e. with no anomalous proper motion, simply by:

$$\mu_\alpha cos\delta \;=\; + w_x sin\delta cos\alpha \;+\; w_y sin\delta sin\alpha \;-\; w_z cos\delta; \qquad \mu_\delta \;=\; - w_x sin\alpha \;+\; w_y cos\alpha$$

A simulation presented by F. Mignard (2003), based on the Véron & Véron list of quasars (2001), shows that the non-rotation condition can be fulfilled to better than 1μas using a number of sources of the order of the ICRF (Figure 6). In the comparison, an additional noise of 20μas was included for source jitter. Notice that such noise would surpass the astrometric accuracy for sources brighter than the 15^{th} magnitude.

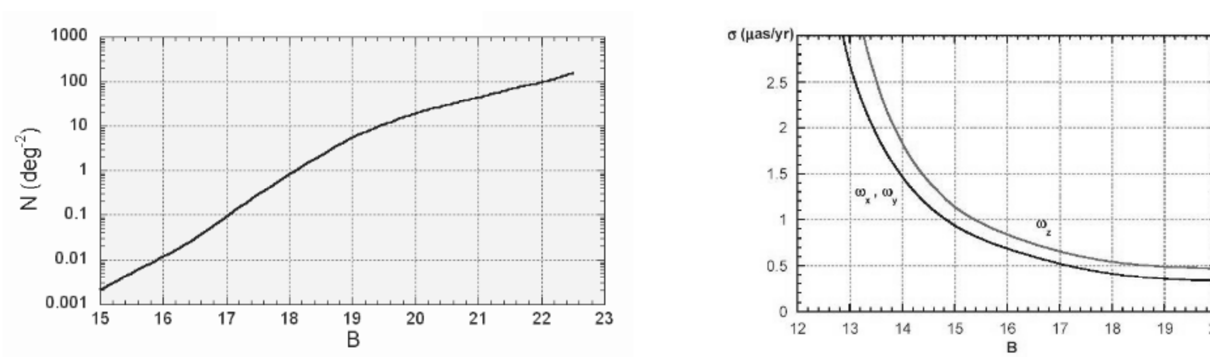

Figure 6. On the left, the quasars' surface density, from Hartwick and Schade (1990). On the right, the relation between the value of the GAIA primary frame global rotation (using galactic coordinates) and the magnitude of the quasars entering in its composition (from Mignard, 2003). The quasar distribution is from Véron & Véron (2001) and is reported as the cause for the worse result for w_z.

The small number of quasars required, if not to define, but certainly to consistently represent the primary GAIA frame, prompts to verify the limits of the continuity for the relative orientation between the present realization of the ICRF and the one formed by the GAIA primary frame. It has been verified that the mean magnitude of the current ICRF's optical counterparts is about B=18. The typical position errors for the VLBI sources are about 0.4mas. Therefore taking the 212 defining ICRF sources and assuming that the error budget is dominated by the ICRF uncertainties, a value of about 50μas is found for the error in the origin offset between the VLBI and GAIA realizations of the ICRF.

A related question, naturally, refers to reasonable values for the "jitter"—spurious or systematic in nature—in the GAIA astrometric quasar measurements. Image centroiding problems can arise from different causes (e.g., underlying galaxy, imperfect instrumental chromaticity correction, even due to macrolensing), but would not result in long-term astrometric biases. On the other hand, random proper motions due to relativistic jets or more generally due to extra-core sub-milliarcsecond instabilities are not undisputedly understood yet. They could reach values of up to 500μas/year, thus posing an issue especially for the reconvening with the ICRF because of the limited number of sources. The main causes of non-erratic, non-globally systematic displacements can be expected to be:

- microlensing, due to galactic stars, typically smaller than 0.1μas/year;
- macrolensing, due to intervening galaxies, seldom larger than 10μas/year;
- systematic proper motions of 4μas/year, on average, due to the galactocentric acceleration of the Sun (Kovalevsky, 2005).

A non-negligible, systematic pattern for the quasars follows: a dual rotational field around the direction pointing towards the galactic center. That is, the maximum proper motion of 5μas/yr occurs at 90° away from the direction of the galactic center and vanishes at the galactic center direction, with no displacement at all.

For all its crucial importance for the basis of the GAIA astrometric frame, quasars represent only a fraction of around 0.0005% of the population of observed objects. Ways to detect the quasars in the population are: by the recognition of known quasars, by the absence of a parallax, by negligible proper motion (in the non-rotating frame), by short term variability, by the spectral signature (from the colors derived by the broad band and from the medium band photometers), by the radial velocity (for the few bright ones, directly by the radial velocity instrument, or as photometric redshift in the majority of cases). All criteria can be used, but there is a trade-off between completeness and efficiency. Completeness will be attained for the sake of the science objectives, in spite of a fraction of contaminants that can be spotted in a later analysis. Efficiency, in the sense of obtaining a very clean sample of quasars only, is however a prime demand for establishing the astrometric primary frame.

The efficiency rate to reach is equal or better than 99.95%. To this level, for example, parallaxes and proper motions should keep mainly a confirmatory role. The same is true for the radial velocity measurements, which mostly will be a part of the spectral energy distribution given by the photometric measurements. In particular, Mignard (2005b) discusses the power of parallax and proper motion tests, and conclude that their combination can be efficient to get rid of nearby stellar contaminants.

The recognition of known quasars finds its best exemplification in the ICRF (Ma et al., 1998; IERS, 1999; Fey et al., 2004), the 11^{th} edition of the V&V list (Véron-Cetty and Véron, 2003), and the recently released SDSS DR4 quasar catalog (Adelman-McCarthy et al., 2006). For these databases, the apparent magnitudes and redshift limits are comparable to the ones within GAIA's reach, while other aspects must be considered more carefully, like the quantity of sources, their sky distribution, and the reliability of the identification. Figure 7 shows the sky distribution and lists the total numbers for the three databases. The ICRF sky distribution is the most even, but the sources quantity is the smallest. However, it is very likely to be used for the sake of continuity between the VLBI's and GAIA's realizations of the ICRS. Since the optical counterparts of the ICRF sources will provide adequate astrometric measurements for the most part, they could be used as a step to define GAIA's frame w residual rotation. The SDSS project covers about one quarter of the sky, permitting a useful test of GAIA's recognition scheme in these areas. The V&V list presents both adequate sky distribution and quantity of objects, though not homogeneity of coverage. It represents a compilation of results from more than a hundred of independent surveys, and a careful assessment of the individual points' reliability has to be envisaged for the degree of cleanness required to establish GAIA's primary frame.

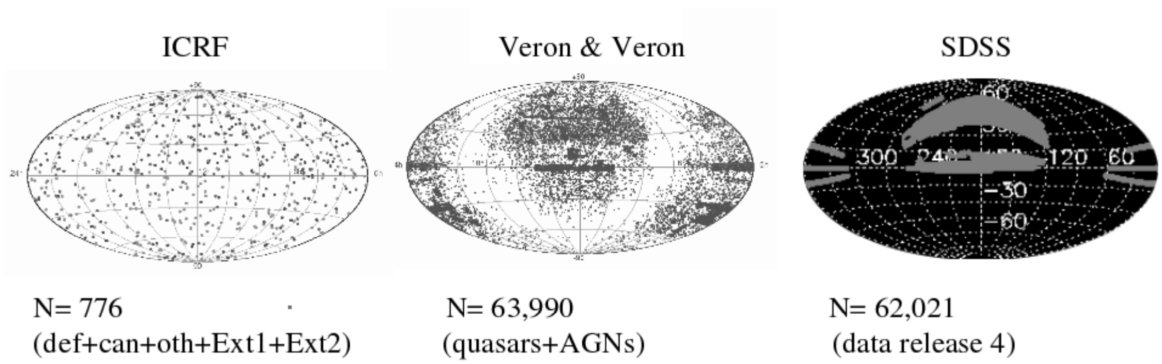

Figure 7. From left to right, the sky distribution of the most recent versions of the ICRF, of the Véron-Cetty & Véron list, and of the Sloan Sky Digitized Survey (SDSS). The plots include all sources that can potentially be used in GAIA's primary astrometric frame (e.g., the defining and candidate sources of the ICRF, quasars and AGNs for V&V). The total numbers are also given.

It becomes clear that in order to establish a large, well-distributed, and even set of quasars, GAIA will have to rely on internal strategies of quasar recognition. For G=20, the star/quasar ratio is about 1,500 in the galactic plane, but it decreases to a tenth at 60° galactic latitude. Besides the evident problems to observe quasars through the Milky Way, the added difficulty to distinguish them therein indicates a zone of avoidance within some 25° from the galactic plane. The most complete way of internal recognition of quasars by GAIA is through the photometric measurements carried out with the broad band and the medium band photometers. Claeskens and collaborators (2004) have generated a large library of synthetic spectra for the quasars, covering a wide range of redshifts, reddening and line strengths. Using in parallel spectral libraries for stars of every spectral class and type, binary stars and white dwarfs, they have correlated all these energy distributions with the different filters proposed for GAIA. Tests were conducted with templates to simulate the observations with realistic noise, and the quasars' locus in the colour space was well defined. By crossing the quasar's synthetic spectral energy distribution with GAIA's proposed photometric systems (Jordi, 2003d), Claeskens and collaborators (2006) have conclusively shown that the combination of the broad band and medium band filters permits a photometric identification of quasars from virtually any type of stars, provided the bands overlap, that they are broad enough to cover the Lyα line and have good spectral coverage. Using only the broad band colors makes it quite difficult to distinguish quasars with $z<2$ from white dwarfs, a traditional contaminant in color-selected quasars. Another ambiguity comes from main sequence stars for quasars at $2.5<z<3.5$. But this can be resolved with the medium band colors thanks to a better sensitivity to the Lyα line. A more difficult case appears with very reddened stars, but these will mainly be confined to the strong absorption region in the vicinity of the galactic plane, where quasars will not be collected for the primary astrometric frame. The photometric redshift can be retrieved as well, even if the actual spectral index differs significantly from that of the template used for the analysis.

GAIA will observe repeatedly each quasar and determine its location in the multi-dimensional color space. In this space, as discussed, they should occupy a different location from that of the stars, including white dwarfs. The GAIA internal, autonomous multi-color detection will be very efficient and will permit the selection of a 99.6% star-free sample of quasars. At G=19, 85% of the quasars are correctly identified with the level of stellar contaminants smaller than 0.01% (0.4% at G=20). Therefore, by reducing the level of completeness of the quasar sample it is possible to virtually eliminate any contaminants. Such a clean sample should contain about 15% of the quasar population, which still amounts to more than 50,000 sources. This is large enough to tie GAIA's astrometric solution to the non-rotating Universe.

4. Acknowledgements

GAIA is a project of the European Space Agency (ESA) with guidance from the scientific community organized into several working groups, coordination units and working packages, all under the auspices of the GAIA Science Team (GST). It is through the efforts of these people, ESA staff and the industrial partners that GAIA has reached its present advanced stage of development. Much of this article has drawn from the GAIA Concept and Technology Study Report (ESA 2000), complied by the former GAIA Science Advisory Group, and from the GAIA Information Sheets, which can be found at http://www.rssd.esa.int. More detailed information and references can also be obtained at that URL. I would like to acknowledge that a lot of information used in the presentation at the IVS General Meeting was gathered from recent presentations by F. Mignard (2005c).

References

[1] Adelman-McCarthy, J.K., Ageros, M.A., Allam, S.S., Anderson, K.S.J., Anderson, S.F., Annis, J., Bahcall, N.A., Baldry, I.K., Barentine, J.C., Berlind, A., and 131 coauthors, 2006, ApJS, 162, p38A.

[2] Arenou, F., 2003, "On-board Data Handling", in GAIA - Taking the Galactic Census.

[3] Bailer-Jones, C.A.L., 2005, Proc. of IAU Colloquium 196 (Cambridge University Press), ed. D.W. Kurtz, p.429.

[4] Bastian, U. and Hefele, H., 2005, Proc. of the Gaia Symposium "The Three-Dimensional Universe with Gaia" (ESA SP-576), ed. C. Turon, K.S. O'Flaherty, M.A.C. Perryman, p215.

[5] de Bruine, J., 2003a, "Scanning Law", in Gaia - Taking the Galactic Census.

[6] de Bruine, J., 2003b, "Astrometric Accuracy Assesment", in Gaia - Taking the Galactic Census.

[7] Claeskens, J.-F., Smette, A., and Surdej, J., 2005, Proc. of the Gaia Symposium "The Three-Dimensional Universe with Gaia" (ESA SP-576), ed. C. Turon, K.S. O'Flaherty, M.A.C. Perryman, p667.

[8] Claeskens, J.-F., Smette, A., Vandenbulcke, L. and Surdej, J., "Identification and redshift determination of QSOs with medium band photometry: application to GAIA", 2006, to appear in Mon.Not.Roy.Ast.Soc.

[9] ESA, 2000, "GAIA: Composition, formation and evolution of the Galaxy", ESA-SCI(2000)4.

[10] Fey, A.L., Ma, C., Arias, E.F., Charlot, P., Feissel-Vernier, M., Gontier, A.-M., Jacobs, C.S., Li, J. and MacMillan, D.S., 2004, Astron.Jour., 127, p3587.

[11] Hartwick, F.D.A. and Schade, D., 1999, Ann.Rev.Astron.Astrophys., vol28, p437.

[12] Hog, E.., 2003, "Sampling in the Astro Telescope", in Gaia - Taking the Galactic Census.

[13] IERS, 1999, "1998 IERS Annual Report", ed. D. Gambis, Observatoire de Paris, p. 87.

[14] Jordi, C., 2003a, "Astro Focal Plane", in Gaia - Taking the Galactic Census.

[15] Jordi, C., 2003b, "Astro Telescope", in Gaia - Taking the Galactic Census.

[16] Jordi, C., 2003c, "Photometric Objectives", in Gaia - Taking the Galactic Census.

[17] Jordi, C., 2003d, "Photometric Systems", in Gaia - Taking the Galactic Census.

[18] Katz, D., 2005, "Spectro Telescope", in Gaia - Taking the Galactic Census.

[19] Katz, D., 2003, "RVS Measurement Principle", in Gaia - Taking the Galactic Census.

[20] Kovalevsky, J., 2005, Proc. of the Gaia Symposium "The Three-Dimensional Universe with Gaia" (ESA SP-576), ed. C. Turon, K.S. O'Flaherty, M.A.C. Perryman, p675.

[21] Lindegren, L., 2005, Proc. of the Gaia Symposium "The Three-Dimensional Universe with Gaia" (ESA SP-576), ed. C. Turon, K.S. O'Flaherty, M.A.C. Perryman, p29.

[22] Ma, C., Arias, E.F., Eubanks, T.M., Fey, A.L., Gontier, A.-M., Jacobs, C.S., Sovers, O.J., Archinal, B.A., Charlot, P., 1998, Astron.Jour., 116, p516.

[23] Mignard, F., 2002, EAS Pub. Ser., vol. 2, Proc. of "GAIA: A European Space Project", ed. O. Bienaym and C. Turon, p327.

[24] Mignard, F., 2003, "The International Celestial Reference System: Maintenance and Future Realization", 25^{th} meeting of the IAU, Joint Discussion 16.

[25] Mignard, F., 2005a, "The L2 Orbit", in Gaia - Taking the Galactic Census.

[26] Mignard, F., 2005b, "Contribution of astrometry to QSO recognition with GAIA", 6^{th} meeting of the GAIA Reletivity and Reference Frame Working Group.

[27] Mignard, F., 2005c, Proc. of "Journes 2004 - systmes de rfrence spatio-temporels. Fundamental astronomy: new concepts and models for high accuracy observations", ed. N. Capitaine, p196.

[28] Perryman, M., 2003a, "Measurement Principle", in Gaia - Taking the Galactic Census.

[29] Perryman, M., 2003b, "Payload Overview", in Gaia - Taking the Galactic Census.

[30] Perryman, M., 2003sc, "Mission Timeline", in Gaia - Taking the Galactic Census.

[31] Véron-Cetty, M.-P.; Véron, P., 2001, Astron.Astrophys., 374, p92.

[32] Véron-Cetty, M.-P.; Véron, P., 2003, Astron.Astrophys., 412, p399.